land

MDPI

Article

Performance Evaluation of TEROS 10 Sensor in Diverse Substrates and Soils of Different Electrical Conductivity Using Low-Cost Microcontroller Settings

Athanasios Fragkos, Dimitrios Loukatos, Georgios Kargas * and Konstantinos G. Arvanitis

Department of Natural Resources Management and Agricultural Engineering, Agricultural University of Athens, 75 Iera Odos Str., 11855 Athens, Greece; athfrag@aua.gr (A.F.); dlouka@aua.gr (D.L.); karvan@aua.gr (K.G.A.)
* Correspondence: kargas@aua.gr

Abstract: This study sheds light on the performance of the common high-precision electromagnetic sensor TEROS 10 to estimate volumetric soil water content (θ) from dry to saturation across three different substrates, six different soil types having three different levels of electrical conductivity of soil solutions (EC_w), and in liquids with increasing salinity level under laboratory conditions, by using low-cost but accurate experimental IoT hardware arrangements. This performance was evaluated using statistical analysis metrics such as Root Mean Square Error (RMSE). It was found that TEROS 10 performance did not conform to the manufacturer's specifications throughout the full scale range, although in some cases good water content estimation was provided. Some inconsistencies were identified by applying the manufacturer's calibration equations, and thus recommendations for improvements are provided, aiming to enhance the sensor's overall performance. TEROS 10 performance across all six soils and three substrates was improved on average from an RMSE of 0.052 and 0.078 cm^3 cm^{-3}, respectively, by using factory-derived calibration, to 0.031 and 0.031 cm^3 cm^{-3} by using the multipoint calibration method (CAL). Furthermore, a linear calibration formula, using Raw output as the predictor variable, was tested and resulted in an RMSE of 0.026 and 0.046 cm^3 cm^{-3} for soils and substrates, respectively.

Keywords: TEROS 10; electrical conductivity; apparent dielectric permittivity; soil moisture; calibration; microcontroller-based measurements; resource preservation; precision agriculture

check for updates

Academic Editor: Cezary Kabala

Received: 22 December 2024
Revised: 21 January 2025
Accepted: 22 January 2025
Published: 24 January 2025

Citation: Fragkos, A.; Loukatos, D.; Kargas, G.; Arvanitis, K.G. Performance Evaluation of TEROS 10 Sensor in Diverse Substrates and Soils of Different Electrical Conductivity Using Low-Cost Microcontroller Settings. *Land* **2025**, *14*, 242. https://doi.org/10.3390/land14020242

Copyright: © 2025 by the authors. Licensee MDPI, Basel, Switzerland. This article is an open access article distributed under the terms and conditions of the Creative Commons Attribution (CC BY) license (https://creativecommons.org/licenses/by/4.0/).

1. Introduction

The accuracy of soil water content data plays a key role in acting and right decision making for plant growth, soil health, automatization of irrigation practices by putting water where and when it is needed, and higher crop productivity [1–5]. Accurate volumetric soil water content (VWC) determination helps in the efficient management of irrigation water in order to maximize crop production, to avoid groundwater depletion but also regarding low consumption because the agriculture sector accounts for 80% of consumptive water use, which makes this use a critical issue for the sustainability of natural resources [6]. In this regard, the development of innovative technologies in the areas of electronics, sensors, Internet of Things, robotics, networking and artificial intelligence have revolutionary transformed the agri-food sector, and have provided innovative systems capable of improving productivity and optimizing the use of natural resources. The need for digital transformation in the agri-food industry became more intensive during and after the COVID-19 pandemic [7]. It is crucial that irrigated agriculture adjusts to the new circumstances, which include drought and extended wetness, as well as the growing global population and its

impact on food demand. The limitation of water resources requires ensuring the needs of plants are met with the least possible water consumption, and optimum irrigation in all parts of the field also ensures improved nutrition and uniform growth of plants.

A widely used method to obtain information about the soil moisture regime is the Time Domain Reflectometry (TDR) method, which is based on the high apparent dielectric permittivity (ε_a) of water, which is 80, whereas the equivalent value of dry soil is in the order of 3 to 7. This great difference of dielectric values between water and dry soil makes the ε_a very sensitive to θ. TDR uses changes in travel time of wave propagation to measure the dielectric constant of a soil, which is related to soil moisture content. The speed at which high-frequency electromagnetic (EM) waves move through a material depends on the material's dielectric permittivity. The TDR method is much less sensitive to factors that could affect the measurement of soils' apparent dielectric permittivity, i.e., organic matter, soil salinity, and clay content, grace to its high operation frequency (*f*) [8,9].

These dielectric measurements could be used to accurately predict the θ using the TDR method. Topp et al. [8] presented a third-order polynomial equation that relates dielectric permittivity to volumetric water content with reasonable accuracy for a wide variety of soils. It has been proven that the square root of apparent dielectric permittivity is a linear function of soil water content [10,11], and so the TDR data convert to θ through the dielectric mixing formula [12].

The dielectric methods are widely accepted but their efficacy can be improved, i.e., ensuring the precise measurement of θ by considering the influence of bulk electrical conductivity (σ_b) on apparent dielectric permittivity (ε_a) [13–18].

Modern dielectric capacitance sensors, which are characterized by a low operating frequency (*f*), usually less than 100 MHz, low power consumption and innovative structure design exhibit a high performance in sensing θ. They emit an electrical field from the sensing end of the device and detect anything that disrupts this electrical field. Capacitance sensors determine apparent soil dielectric permittivity by measuring the charge time of a capacitor (i.e., the soil-probe system) for a given voltage [19]. Many different sensors' manufacturers claim that their sensors' volumetric water content (VWC) accuracy is between 1% and 2% for almost all soils, and it is productive to focus to the factors that often affect that accuracy and to examine the correctness of this claim [20,21]. Increasing the accuracy of water content measurements means very accurate measurements of dielectric permittivity, but often the apparent dielectric permittivity is affected by bulk soil electrical conductivity (σ_b), and estimation of θ is not always accurate [10]. The next step is the quality of the special calibration of the instrument from detected dielectric permittivity to take VWC measurements as accurately as possible. The development of popular and successful soil moisture sensors has the goals to avoid texture and salinity effects, to have a design that makes it easy for them to be inserted into different soils, and for the sensors to be more durable and accurate in measurements. There are still some areas that could be improved on.

The soil relative complex permittivity, ε^*, can be expressed by the equation

$$\varepsilon^* = \varepsilon_r - j\varepsilon_i \quad (1)$$

where ε_r is the real dielectric permittivity, which expresses the capability to store electric energy, ε_i is the imaginary dielectric permittivity, which represents the energy loss, and $j = \sqrt{-1}$.

If we divide the relation (1) by the dielectric constant of the vacuum $\varepsilon_o = 8.85 \times 10^{-12}$ Fm^{-1} we obtain its conversion to the relation (2)

$$\varepsilon^*_r = \varepsilon'_r - j\varepsilon''_i \quad (2)$$

The imaginary component of the dielectric permittivity is the sum of a conduction term and a relaxation term [10]

$$\varepsilon''_{\mathrm{i}} = \varepsilon_{\mathrm{rel}} + \frac{\sigma b}{2\pi f \varepsilon 0} \tag{3}$$

where $\varepsilon_{\mathrm{rel}}$ is the molecular term, which in most soils is small, σ_{b} is the electrical conductivity (EC) and $\varepsilon_0 = 8.85 \times 10^{-12}$ Fm^{-1}.

Any material that is able to store electrical charge has a unique ability, referred to as its dielectrical constant, which is the ratio between ε_{r} and ε_0 and expresses how much energy can be stored by the electromagnetic field that is imposed. The dielectric constant is mainly related to soil moisture, θ, as well as to the spatial distribution of the soil's liquid phase [10,22]. Meanwhile, the imaginary part, $\varepsilon''_{\mathrm{r}}$, refers to the quantity of the dielectrical material's inherent dissipation of electromagnetic energy, which takes place when the charges inside the material reorient because of the application of an electric field. The polarization expresses the capacity of the water in soil to oppose an electrical field that is applied to it. At lower frequencies, sensors polarize the water and the dissolved salts make them very sensitive to salinity in the soil [9]. At higher frequencies, this phenomenon weakens but at the same time increases sensors' cost. The various polarization mechanisms appear in different critical frequencies, known as relaxation or resonance frequencies. As the frequency increases, the "slower" mechanisms drop out, leaving the faster ones contributing to energy storage. The imaginary part of the dielectric constant, mentioned above, will take its maximum value for each critical *f*. Polarization of water molecules or dissolved ions is the rearrangement of charges inside the material, opposing the external electric field that is applied. Dipole orientation takes some time because a material's polarization does not change instantaneously when an electric field is applied. At a critical frequency, the dipoles cannot follow the changes, and response time becomes slower. As a result, the dielectric constant is reduced by the frequency. Selecting dielectric devices at high frequencies is important to obtain the right response [9,10].

Frequency dispersion is the phenomenon where the dielectric constant and dielectric losses vary with applied frequency, *f*. The frequency range in which a soil sensor operates is very critical for its behavior. The real part of the relative apparent permittivity appears to obtain the largest values at low operation frequencies and generally tends to decrease with increasing frequency [8].

Due to the number of the aforementioned parameters that affect apparent permittivity or could give inaccurate measurements, it is critical to develop technologies to avoid or at least to minimize the effect of these factors on the measurements and the sensor's performance.

Ferre and Topp [9] proposed an equation that expresses the relationship between θ and ε_{a}, and showed that soil water content is calculated from ε_{a} using a simple regression formula that relates θ to ε_{a} using the general form

$$\theta = \mathrm{a}\sqrt{\varepsilon_{\mathrm{a}}} + \mathrm{b} \tag{4}$$

where a and b are fitting parameters. Equation (4) represents a simplification of the physically based Complex Refraction Index Model (CRIM), with an additional term denoting bound water fraction [14].

Topp and Reynolds [12], using the form of Equation (4), have shown that for TDR the following governing equation,

$$\theta = 0.115\sqrt{\varepsilon_{\mathrm{a}}} - 0.176 \tag{5}$$

is effectively equivalent to the third-order calibration equation developed by Topp et al. [8], and it deviates less than 0.01 m^3 m^{-3} over a θ range 0.05 to 0.45 m^3 m^{-3} for the TDR measurements.

The existence of a corresponding linear relationship, $\theta - \varepsilon^{0.5}$, has been demonstrated for many dielectric sensors. The high clay content, the organic matter and the salinity level can alter the value of slope a (Equation (4)) and may introduce curvature [22]. Dense soils may have an impact on the value of interception b (Equation (4)) given that the magnitude of that term is dependent on the soil solids composition. These values are also affected by the type of soil, the operating frequency of the sensor, the temperature, the bulk soil electrical conductivity and the special characteristics of the sensor [13].

However, the question remains whether the linear relationship $\theta_m - \varepsilon^{0.5}$ is valid for TEROS 10 device (from Meter Group AG, Pullman, WA, USA) in many types of soil, whether the accuracy of the sensors is affected and how the values of parameters a and b are influenced by changes in soil salinity. Peranic et al. [23] examined the hydraulic monitoring of downscaled slope models under simulated rainfall in a laboratory environment using TEROS 10, among other sensors. The results demonstrated the need for performing a specific calibration in a scaled slope model. Millan et al. [24] evaluated the performance of six moisture sensors including TEROS 10 in sandy soil, and proposed a third-order polynomial equation that corrected the θ value from the manufacturer's calibration by adding some parameters. Both equations demonstrated similar behavior with low soil moisture content, and the factory equation overestimated soil moisture values above a moisture level of 0.10 cm^3 cm^{-3}. Cominelli et al. [25] determined the sensing volume of TEROS 10, along with the TEROS 12 sensor, and found differences between obtained values for both sensors from the reported support volume by the manufacturer in some cases such as in dry sand, in moist sand and in water. Moreover, the most interesting point of this study was that a single linear equation (θ − Raw) for all soil types was proposed, using the raw values to predict θ, and it evaluated the temperature sensitivity of both sensors for all soil types. This linear equation (θ − Raw) provided better performance compared with the polynomial factory-based model (θ − Raw^3), which fitted better only to θ < 0.1 cm^3 cm^{-3} and to θ > 0.4 cm^3 cm^{-3}. As two different soil samples were exposed at temperatures ranging from 2 °C to 40 °C, there were no considerable changes in VWC measurements. Nasta et al. [14] presented a linear temperature-corrected calibration, which outperformed temperature-independent factory calibration for clay and loam soil, and they noted that the parameter values a and b of the linear equation $\theta_m - \varepsilon^{0.5}$ were different for each soil type due to the influence of temperature.

The objectives of this research are (a) to validate and examine the precision of the suggested third-order polynomial calibration equations for the TEROS 10 sensor in various soil types and substrates, as given by the manufacturer, (b) to investigate its response in aqueous solutions with different EC and (c) to compare the models using $\theta_m - \varepsilon^{0.5}$ (Equation (4)) or Raw [23] or Raw^3 (manufacturer-based third-order calibration equation) outputs as the predictor variable for more accurate estimation of θ. Moreover, a specific objective of this study is to compare and evaluate the performance of the multipoint calibration $\theta_m - \varepsilon^{0.5}$ (CAL) approach against the manufacturer's calibration across a range of soil types, substrates, moisture conditions and salinity conditions. The multipoint calibration procedure (CAL) is used to determine a and b parameters in Equation (4) through linear regression, and is applied on all experimentally measured volumetric soil water (θ_m) values.

2. Materials and Methods

2.1. Sensor Characteristics

The TEROS 10 sensor from Meter Group AG measures indirectly the Volumetric Water Content in any soil, as well as the apparent dielectric permittivity of the porous media, by applying a 70 MHz signal, an operation frequency that minimizes salinity and textural effects. TEROS 10 has two stainless steel needles, 5.5 and 5.1 cm long each, respectively, which glide into any soil and can easily be integrated into a wide variety of data-collecting systems. There is no need for wiring or programming and it operates on a capacitance-based technique through which the steel rods acts as a capacitor and the soil-surrounding area acts as a dielectric medium. The sensor has an epoxy body to make it more durable and able to survive better in tough field conditions and also a ferrite core to eliminate cable noise. It is designed to be rugged enough in order for the needles not to break under harsh soil circumstances, and it is optimized for easier installation and for continuous field measurements. Streamlining the calibration process allows for a better performance of the sensor. The sharpened needles, which have very sharp tips, can be installed easily in hard soils, i.e., clays, and have an embedded thermistor and hard plastic body, which make them less susceptible to breaking. To improve the accuracy and the overall performance of the sensor to ensure better exploitation of its potential, a custom calibration should be performed in order to obtain accurate and reliable data.

As far as TEROS 10 is concerned [26], RAW values, which are measured in mV, are converted to VWC by the following calibration equation specific to mineral soils

$$\theta\ (\mathrm{cm}^3/\mathrm{cm}^3) = 4.824 \times 10^{-10} \times \mathrm{mV}^3 - 2.278 \times 10^{-6} \times \mathrm{mV}^2 + 3.898 \times 10^{-3} \times \mathrm{mV} - 2.154 \quad (6)$$

converted to VWC by the next calibration equation specific to soilless media

$$\theta\ (\mathrm{cm}^3/\mathrm{cm}^3) = 5.439 \times 10^{-10} \times \mathrm{mV}^3 - 2.731 \times 10^{-6} \times \mathrm{mV}^2 + 4.868 \times 10^{-3} \times \mathrm{mV} - 2.683 \quad (7)$$

and converted to dielectric permittivity by the equation below

$$\varepsilon = 1.054 \times 10^{-1} \times \mathrm{e}^{2.827 \times 0.001 \times \mathrm{mV}}. \quad (8)$$

The TEROS 10 sensor estimates volumetric water content that ranges for mineral soils from 0 to 0.64 $\mathrm{cm}^3\ \mathrm{cm}^{-3}$ with a measuring accuracy $\pm 3\%$ when the electrical conductivity of the solution is EC < 8 dS m^{-1}. The resulting measurement volume of TEROS 10 is about 430 cm^3. The output signal of TEROS 10 is analog and ranges from about 1000 to 2500 mV. This instrument requires DC voltage between 3.0 V and 15.0 V to operate properly, while its nominal power consumption is 12.0 mA, approximately. The sensor is compatible with most data logging systems, its cost is comparatively low and its usage is simple.

In addition, Cominelli et al. [25] in a recent study proposed a new single calibration equation, based on Raw output, as the predictor variable, using the formula

$$\theta\ (\mathrm{cm}^3/\mathrm{cm}^3) = 4 \times 10^{-4}\mathrm{RAW} - 4.102 \times 10^{-1}. \quad (9)$$

2.2. Technical Arrangements for Data Collection and Processing

In line with the analysis presented in Section 3.1, reliably collecting the data provided by TEROS 10 presupposes electronic equipment that is adapted to the output characteristics of this soil instrument and is also able to process and deliver the harvested data to the final user. These tasks can be addressed by either commercial or custom data logging systems, with the latter to be less expensive and open to tailoring/modifications implied by the diverse experimental research settings. In this regard, a properly adapted version of the platform initially presented in [27] and refined in [28] was utilized in this study,

exploiting the potential of the Atmel 32u4 microcontroller, equipped with communication options via a USB port and/or a LoRa transceiver chip. TEROS 10 was power cycled, and its voltage output was digitized by the analog-to-digital converter (ADC) module of the microcontroller, while the corresponding quantities of interest (i.e., θ and ε values) were extracted through the proper arithmetic post processing.

The generic wiring diagram of the electronic components necessary for reading the data from the different soil instruments is given in [28]. As explained therein, a dual 4-channel analog multiplexer/demultiplexer module (i.e., a 74HC4052 chip by NXP Semiconductors, Petaling Jaya, Malaysia) is utilized to power cycle and acquire the data from the diverse soil instruments, while the excessive current and voltage required by each sensor are provided to a controllable DC-DC converter module (an MiniBoost 5V @ 100mA Charge Pump by Adafruit, New York, NY, USA). There is provision for connecting and powering instruments of either analog or digital output. In case of analog instruments, like TEROS 10, the comparatively low native 10 bit resolution of the ADC of the Atmel 32u4 microcontroller is increased by performing oversampling 16 times, via software. According to the manufacturer specifications of the soil instruments, the improved 12 bit resolution equivalent outcome is fluent for data recording. It should also be noted that, as explained in [28], utilizing an accurate analog reference voltage chip (i.e., the LM4040 breakout module by Adafruit, New York, NY, USA), the linearity of the ADC module of the 32u4 microcontroller and its tolerance to temperature variations are satisfactory, despite its low price. The only imperfection is that the specific microcontroller does not generate exactly 3.30 V and 2.56 V analog reference values, as expected, but (in our case) 3.29 mV and 2.54 mV. Consequently, these values should be used inside the ADC conversion formulas, to provide calibrated and more accurate results.

Throughout the experiments, the necessary measurement inspection/collection was carried out via the USB port of the system, which was connected to a conventional computer/laptop and a serial console monitoring application like the Serial Monitor tool provided by the Arduino IDE environment. This arrangement was satisfactory for a wide variety of cases, which have already delivered encouraging results [27,29]. As the main sensor node, supported by the Feather 32u4 LoRa board (manufactured by Adafruit, New York, NY, USA) could also communicate with a Raspberry Pi (RPi) unit (manufactured by Raspberry, Pencoed, UK), wirelessly via LoRa, more options existed for permanent storage of the data and for post processing. This feature was very useful during the experiments that required a long period of measurements and/or complement with auxiliary data, in pace with the soil-specific ones.

Indeed, the specific system was utilized to provide automated gravimetric soil moisture data, in parallel with the recordings of the TEROS 10 capacitance-based instrument, in case of stone wool sub-traces. As explained in [29], the apparatus used for the specific experiment consisted of a small plastic container, a sample of stone wool, a digital camera, a precision scale, a temperature/humidity sensor and the aforementioned sensor node. TEROS 10 was placed in the plastic container, along with the stone wool and the microcontroller board. The stone wool's net weight was initially measured and, to obtain the maximum moisture level, the stone wool sample was entirely immersed in fresh water, while the moisture sensor was placed horizontally inside the left side of the sub-trace. The periodic soil moisture measurements sent from the sensor node to the RPi unit triggered the digital camera to take a photo, which was also stored into a corresponding time-stamped file inside the micro SD card of the RPi. An auxiliary air temperature and humidity sensor, connected on the 32u4 unit, reported the ambient environment conditions throughout the experiment. Figure 1 illustrates details of the sensor node supporting the data acquisition process from the TEROS 10 instrument.

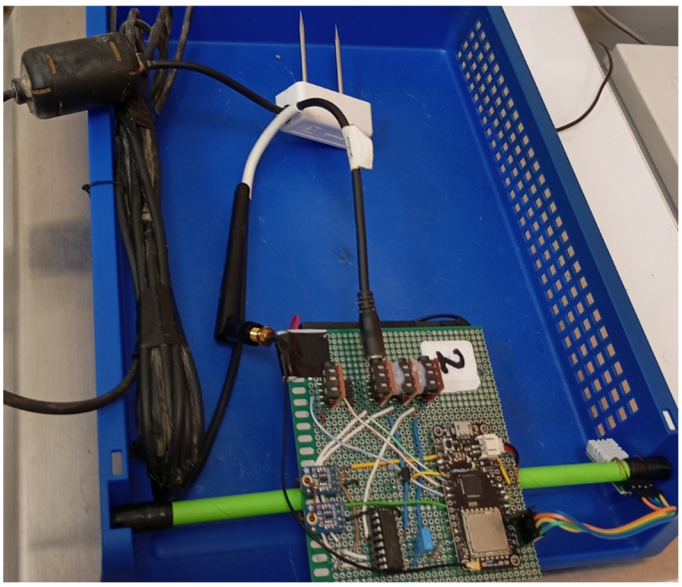


Figure 1. Details of the sensor node supporting the data acquisition process from the TEROS 10 instrument.

2.3. Substrates Properties

Three substrate types, widely used in hydroponic and floriculture applications, were tested in this study to evaluate the performance of TEROS 10. The three substrates are commercial products [30–32]. The experiments were performed in the laboratory facilities of the Department of Natural Resources and Agricultural Engineering at the Agricultural University of Athens, where the temperature remained 22 °C ± 1 °C.

Peat is a natural product that has excellent properties as a soil improvement material. Specifically, it helps the soil retain water, air and nutrients that would otherwise be lost from the soil. Peat has a uniform composition and does not compact, so can last for years in soils and help the soil hold nutrients by increasing what is called the CEC or "cation exchange capacity" [33]. Peat not only improves soil structure and aeration, but it also helps in the development of the root system. Moreover, it has an unlimited lifespan and it is known for its ability to hold 3–4 times its weight in water, offering economy. The sample (Figure 2a) was selected from high-quality Baltic peat moss that had pH varying between 3.5 and 4.5, electrical conductivity (EC) between 0.05 and 0.15 mS cm^{-1}, and organic substrate between 92 and 98%. Prior to the experiment, the sample was initially weighed, then was placed in the oven (60 °C for 48 h) and finally weighed again to verify its water content.

Perlite is a natural occurring, aluminosilicate, volcanic mineral that provides aeration and moisture retention to agricultural crops (Figure 2b). It contains 3 to 4% crystalline water and is of volcanic origin. When it reaches 700–1000 °C, the perlite softens (since it is a glass) and the water, which is trapped in its structure, escapes, and this creates the swelling of the material from 7 to 15 times. The feature makes watering plants more efficient, enhancing water retention in drought conditions, especially in the summer months [34]. The expanded perlite that was used is chemically inert, and has a pH of 7.0–7.5 and a grain size of 1–5 mm; its air content at maximum water retention is 56% and it is used exclusively in agricultural applications.

Stone wool (Figure 2c) is a substrate that is used mostly in greenhouses; it is made from basalt and provides a uniform growing media because it has air pockets that allow the roots to make better use of the substrate. It is known for its water-saving properties, and it uses less water than soil, is pH neutral and 100% recyclable. There are no pathogens in stone wool because it is processed at 1500° C, which ensures a clean and safe growing medium for rapid root system development and optimal growing results. The sample that

was used contained the following properties: pH = 6.9, EC: 50–100 μS cm^{-1} and organic material = 4.5%. The bulk density of each substrate is shown in Table 1.



(**a**) (**b**) (**c**)

Figure 2. Photos from the experimental procedure concerning (**a**) peat, (**b**) perlite, (**c**) stone wool.

Table 1. Soil and substrate properties.

Soil Type	Clay	Silt	Sand	Dry Bulk Density
	%	%	%	(g/cm^3)
Sand			100	1.66 ± 0.01
Sandy Loam	16	11	73	1.24 ± 0.01
Loam	19	32	49	1.23 ± 0.01
Clay	48	12	40	1.13 ± 0.01
Sandy Clay Loam	25	12	63	1.26 ± 0.01
Silty Clay Loam	31	49	20	1.11 ± 0.01
Peat				0.177 ± 0.01
Perlite				0.084 ± 0.01
Stone Wool				0.094 ± 0.01

2.4. Measurement in Soils

Six porous materials, sand, clay, loam, sandy loam, sandy clay loam and silty clay loam, with different characteristics were used in this study to analyze the performance of the TEROS 10 sensor (Table 1). Specifically, they were collected from the Prefectures of Athens and Argolida from agricultural regions, with the exception of sand, which is used as artificial substrate in floriculture. These porous materials were selected because they exhibit a variety of properties such as bulk density, soil texture and porosity. All experiments in this study were performed in the laboratory under constant temperature-controlled conditions (22 ± 1 °C) to avoid temperature effects. The experiments took place in laboratory conditions. The air-dried soil samples were sieved for a particle size ≤ 2mm, and the determination of initial soil moisture was performed through the oven-drying method. A soil sample of each porous material was placed into the oven for 24 h at 100 °C. The dry bulk density of each sample was calculated by simply dividing the dry mass of the soil by the volume of the soil. Water was added to each porous material in a strictly defined manner from dry up to the saturation point in equal water content steps

of $\theta = 0.05$ cm^3 cm^{-3}. Specifically, the volume of the sample was 1500 mL, and 75 mL of fresh water ($EC_w = 0.28$ dS m^{-1}) was added to the sample each time to increase the water content by $\theta = 0.05$ cm^3 cm^{-3}. The soil was mixed until the mixture was homogenous. With a view to homogeneity of density distribution in the soil sample, the obtained soil material was pressed with a 0.20 kg hammer at various water content levels. For all soils, three wetting solutions were used, with EC_w values of 0.28, 6 and 10 dS m^{-1}. TEROS 10 was installed vertically into the soil samples and the sensor's outputs were taken. At the end of the experiment, the soil θ_m values and dry bulk density were reassessed by weighing and oven drying. Proper sensor installation was carefully carried out, taking care to minimize air gaps and not inserting the sensor in holes that were already made.

At the same time, it was ensured that the distance between the walls of the container was at least more than the 3 cm required by the manufacturer, so as not to affect the measurements or affect the reading of the sensor. The multipoint calibration CAL was used to receive the values for a and b for the relationship (Equation (4)) between the square root of ε_a and θ_m, using all the measured θ_m values by applying linear regression between θ_m and $\varepsilon_a^{0.5}$. Great emphasis was given during the experimental procedure to measure the same quantity three times, in order to estimate more accurately the actual value of the quantity and determine possible variations for the same measurement.

2.5. Salinity Effects in Water Solutions and Soils

TEROS 10 sensitivity to salinity was validated by carrying out experiments in water solutions and in soils with increased EC_w values. The experiments were conducted using water solutions with increasing electrical conductivity values, EC_w, from 0 to 20 dS m^{-1} by adding potassium chloride (KCL) to deionized water in order to investigate TEROS 10 sensitivity and response to EC_w changes. The focus of this effort was to verify the stability of the sensor's ε_a readings with increasing salinity levels. The sensor was inserted in a vertical position into the liquid solutions, and the captured data were analyzed for various increasing EC_w values. The experiments with the sandy clay loam and silty clay loam were conducted by using solutions with $EC_w = 0.28$ dS m^{-1}, whereas with soil samples of sand, sandy loam, loam and clay, three EC_w levels were used, with values of 0.28, 6 and 10 dS m^{-1}. The steps in the experimental procedure for all soil samples are described in Section 2.4 in detail.

2.6. Measurements in Substrates

For peat, the same methodology was followed as for the soils for the VWC estimation. Specifically, in order to determine the initial moisture, a sample of peat of known mass was placed into the oven for 48h at 60 °C [35], and was weighted before and after it was placed in the oven. The volume of the peat sample was 2500 cm^3, and it was thoroughly mixed with 125 ml of fresh water (EC = 0.28 dS m^{-1}) to increase the water content each time by $\theta = 0.05$ cm^3 cm^{-3} until saturation was reached. The sensor was inserted vertically in the peat sample and the large ferrite core of TEROS 10 was carefully attached in such a place to avoid failures in measurements. The perlite sample was sprayed with fresh water (EC = 0.28 dS m^{-1}) following equal moisture steps of $\Delta\theta = 0.05$ cm^3 cm^{-3} until saturation point, which was $\theta = 0.30$ cm^3 cm^{-3}. The method for the stone wool was simple to perform and did not require much specific technical knowledge. It provided direct measurements of water content and allowed us to calculate available moisture content through the gravimetric method. After completing drying the stone wool sample, it was weighed, then placed on the platform, and the whole system was positioned on the weighing scale. The initial weight of the stone wool was determined. The sample was immersed in a container with tap water to achieve saturation level, which reached

approximately the value of θ = 0.85 cm^3 cm^{-3}. The sensor was inserted in a horizontal position in the middle of one side, as it is shown in Figure 2c. Silicone was used to stick the plastic spacers at the bottom of stone wool to ensure that the evaporation took place from all sides unhindered. The raw data were collected from TEROS 10, recorded on the data logger, as described in detail in Section 2.2, and delivered to the cloud every four hours, along with a captured photo image from the digital camera, which allowed daily continuous observation of the exact moist weight, and we then proceeded to calculate the substrate water content. The experiment was performed using equipment that included a container, a stone wool sample with dimensions 20.5 × 14.4 × 7.1 cm^3, plastic spacers, a data acquisition system, a digital camera and a precision scale.

2.7. Statistical Tools for Performance Evaluation

In order to evaluate the validity of the manufacturer's supplied calibration equations, the metrics of Root Mean Square Error (RMSE) deviation, the correlation coefficient R^2 formula and the Mean Absolute Error (MAE) were used. Their mathematical expression is presented below

$$\mathrm{RMSE} = \sqrt{\frac{1}{n}\sum_{i=1}^{n}\left(O_{i-}P_i\right)^2} \tag{10}$$

$$R^2 = \frac{\sum_{i=1}^{n}\left(O_i - P_i\right)^2}{\sum_{i=1}^{n}\left(O_i - \overline{O}\right)^2} \tag{11}$$

$$\mathrm{MAE} = \frac{\sum_{i=1}^{n}\left|x_{exp} - x_{true}\right|}{n} \tag{12}$$

where o is the corresponding observed value, $\overline{O}$ is the observed mean value, P is the predicted value of the modeled parameter, i is the counter for data pairs, x_{exp} is the experimental measurement, x_{true} is the actual value, and n is the total number of different pairs of observed–predicted values for RMSE and R^2 or the total number of observations for MAE. The statistical metric R^2 varies between 0 and 1.

3. Results and Discussion

3.1. Salinity Effects in Liquid Solutions

In Figure 3, it is shown that the TEROS 10 sensor has an irregular behavior, as EC_w increases in aqueous KCl solutions. Specifically, it is much affected by the increase in salinity up to about 3 dS m^{-1}, and from 0 to 3 dS m^{-1} the Raw values decrease to around the value 2200 from an initial value of 2323. The ε_a values, in this range of changes in Raw values, vary from about 76 to 54 if Equation (8) is applied. This response is contrary to what was expected since the manufacturer's guideline reports that the Raw values should not be affected by increasing salinity level up to 8 dS m^{-1}. At about EC_w = 5 dS m^{-1}, the values of Raw increase slightly and they converge after stabilization to a value of about 2345 approximately, with increasing salinity to the value of 20 dS m^{-1} [27,29]. Many researchers reported the contrary behavior of other sensors such as the Hydra Probe sensor, Sigma probe sensor, WET sensor and CS655 sensor (operation frequency 50 MHz, 30 MHz, 20 MHz, 175 MHz, respectively), which use a low-frequency measurement and are not affected as salinity increases up to EC_w = 3 dS m^{-1} [36–38]. Only 5TE and TEROS 12 sensors have a similar response to TEROS 10, as it is reported by Schwartz et al. [17], Kargas et al. [38] and Rosenbaum et al. [39]. The corresponding range of change of ε_a values is from about 54 to 79.

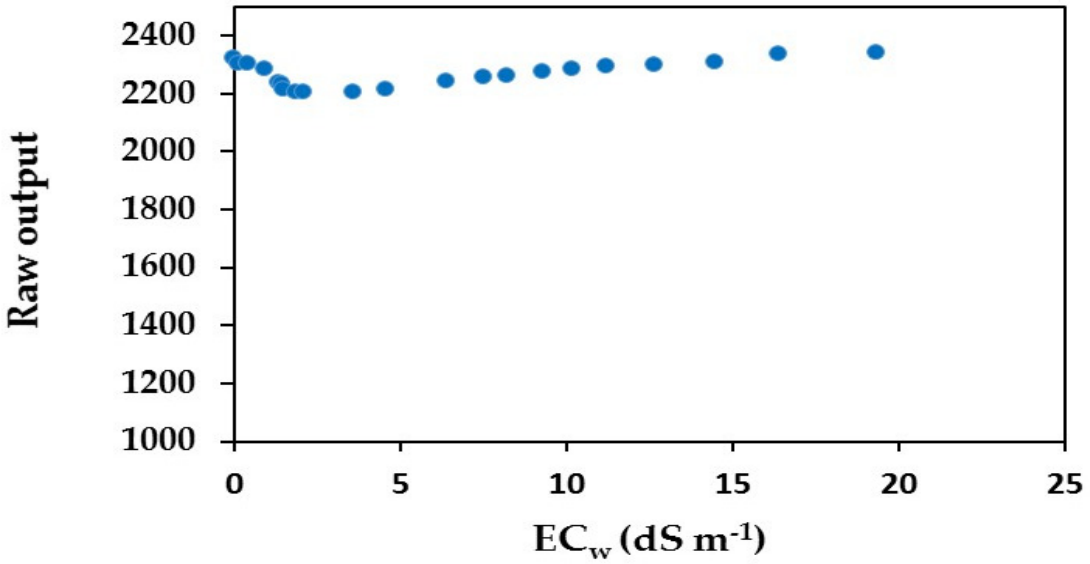


Figure 3. The Raw values against EC_w in aqueous KCL solutions for the TEROS 10 sensor.

3.2. Soil and Substrate Specific Calibration for EC = 0.28 dS m^{-1}

Figure 4 illustrates the ε_a readings, as determined by TEROS 10 (Equation (8)), according to the actual water content (θ_m) of all six soil samples and substrates for EC = 0.28 dS m^{-1} (red points). From the results, it is shown that TEROS 10 gives lower values for ε_a, compared with the ones derived via the Topp equation (Equation (5)) for the same θ_m level for all soil types. From Table 2, it is shown that the $\theta_m - \varepsilon^{0.5}$ relationship is strongly linear for all examined cases ($0.905 < R^2 < 0.993$); meanwhile, the values of parameters a and b deviate significantly from those obtained by the Topp equation (Equation (5)). In addition, the values of these parameters differ between the examined porous media. In Table 2, the corresponding values of RMSE are presented, extracted by applying the CAL method. From the results, it appears that the CAL method significantly improves the estimation of soil water content, θ, taking into account that RMSE < 0.043 cm^3 cm^{-3} in all examined cases (Figure 5); meanwhile, the third-order calibration equations (Equations (6) and (7)) result in RMSE values that range from 0.033 to 0.096 (Table 2). These results show that the CAL method significantly improves the estimation of VWC.

Table 2. Parameters a (slope) and b (interception) in relationships $\theta_m - \varepsilon_a^{0.5}$ for all soil types and substrates, along with R^2 and RMSE values extracted from multipoint calibration (CAL) for EC = 0.28 dS m^{-1}. Additionally, the RMSE values from manufacturer's third-order calibration equation (Manuf. CAL) (Equations (6) and (7), respectively).

Soil Type	b	a	R^2	RMSE (CAL)	RMSE (Manuf. CAL)
Sand	−0.213	0.174	0.964	0.022	0.061
Sandy Loam	−0.155	0.135	0.980	0.018	0.052
Loam	−0.118	0.127	0.905	0.040	0.060
Clay	−0.089	0.080	0.956	0.027	0.046
Silty Clay Loam	−0.129	0.124	0.954	0.028	0.047
Sandy Clay Loam	−0.102	0.094	0.965	0.024	0.033
Perlite	−0.070	0.091	0.923	0.028	0.058
Peat	−0.015	0.108	0.955	0.043	0.081
Stone Wool	-0.113	0.122	0.993	0.022	0.096

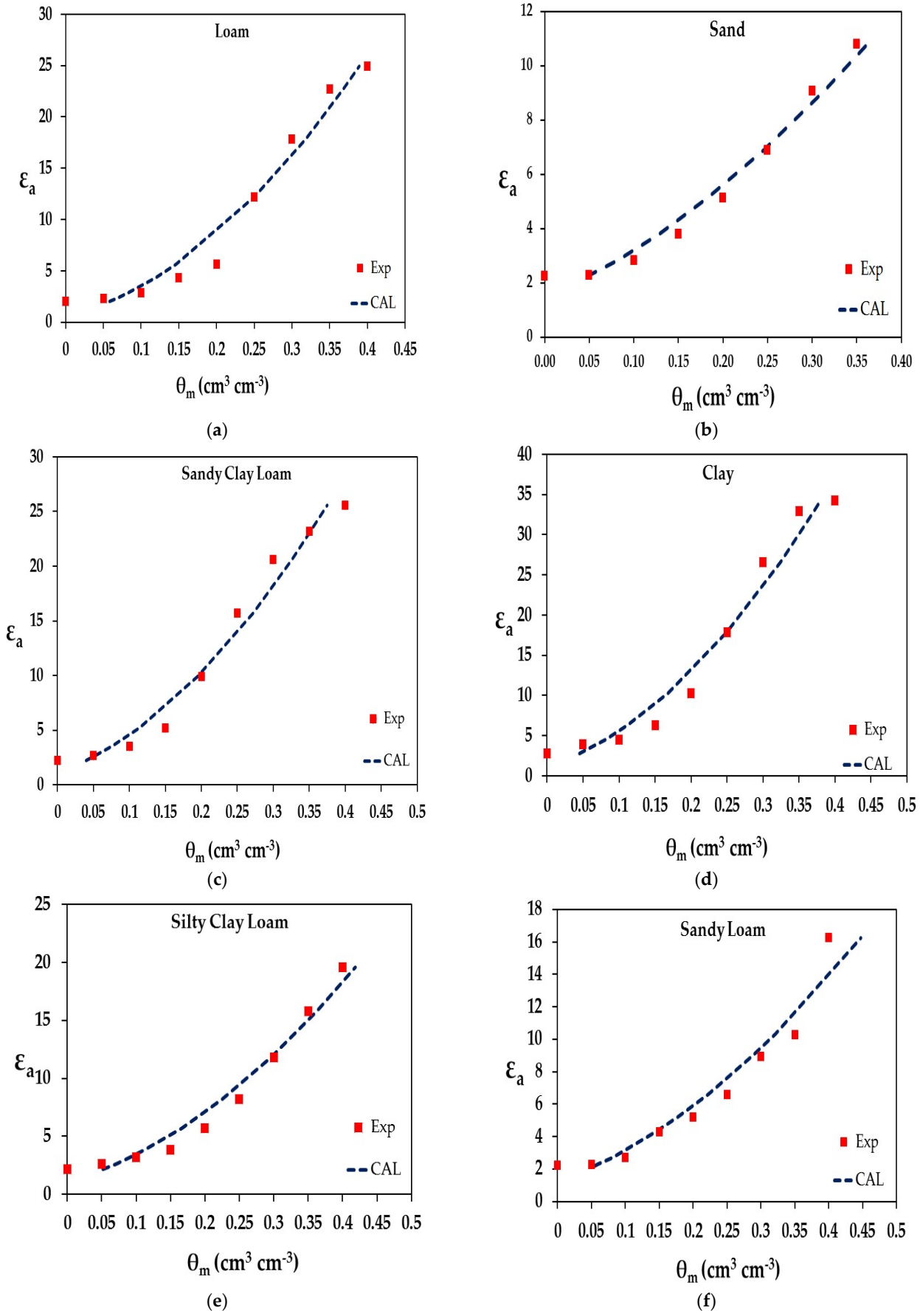


Figure 4. *Cont.*

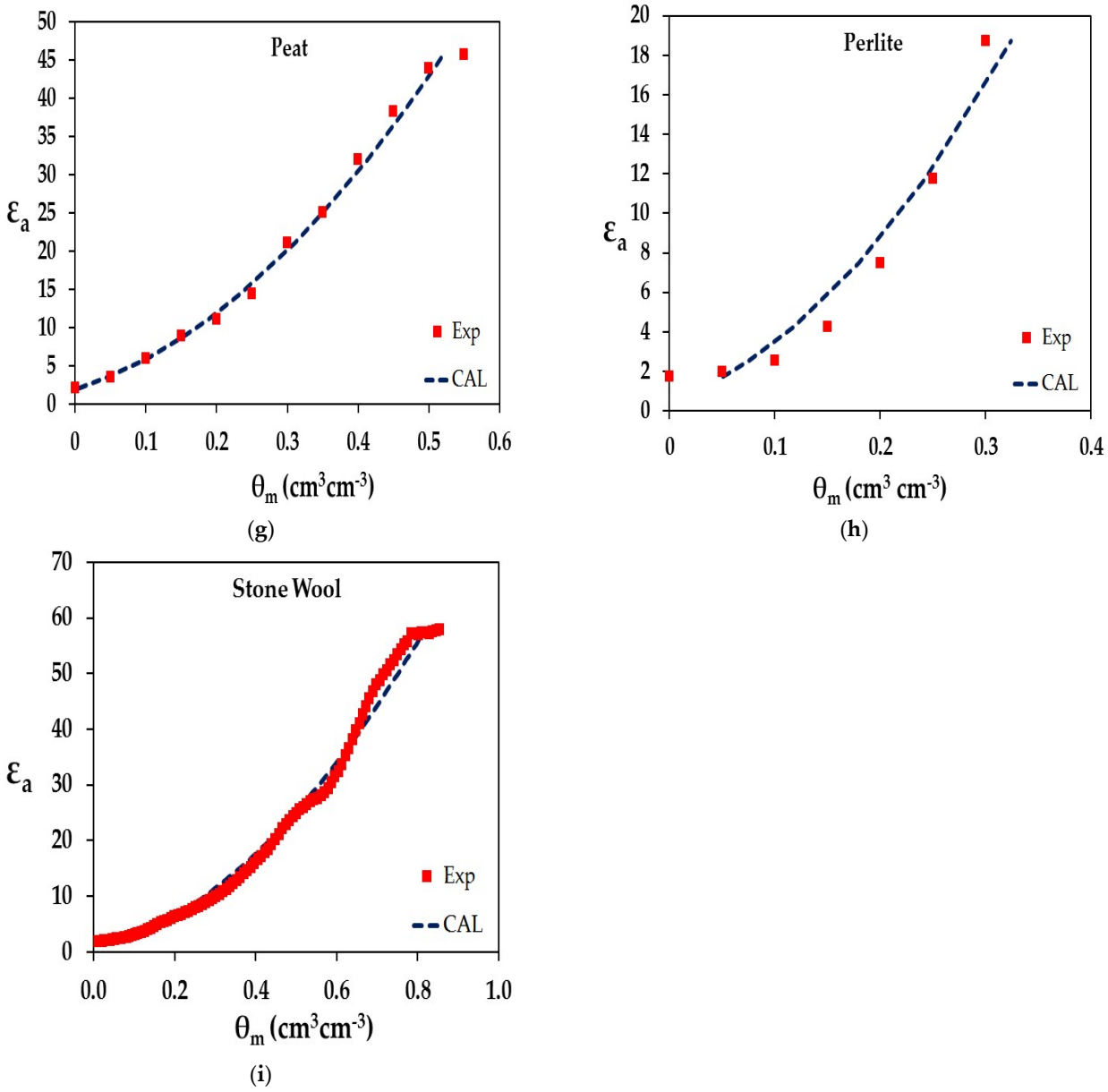


Figure 4. The $\varepsilon_a - \theta_m$ relationship (point) for (**a**) loam, (**b**) sand, (**c**) sandy clay loam, (**d**) clay, (**e**) silty clay loam, (**f**) sandy loam soil, (**g**) peat, (**h**) perlite and (**i**) stone wool samples for measurements with TEROS 10 for EC_w = 0.28 dS m^{-1} (EXP) and also the relationship of $\varepsilon_a - \theta$, where θ is calculated by the soil-specific CAL calibration equation (CAL). The ε_a-θ relationship for the case of CAL is referred to the solution with EC_w = 0.28 dS m^{-1}.

In Table 3, the coefficients a and b of the linear calibration equations $\theta - Raw$ are shown, for all examined soils and substrates at EC = 0.28 dS m^{-1}. Moreover, the R^2 and RMSE are presented for each examined case. The $\theta_m - Raw$ relationships are strongly linear for soils ($0.962 < R^2 < 0.987$), while for soilless porous media they range from 0.887 to 0.963. Cominelli's equation provides better results than the third-order manufacturer's equation, even though it is a single equation for all soil types. From these results, it is shown that the relationship $\theta_m - Raw$ appears to be more linear compared with the linear relationship $\theta_m - \varepsilon^{0.5}$ and provides lower RMSE values, especially in inorganic soils. The RMSE values for linear calibration ($\theta - Raw$) range from 0.017 to 0.028 cm^3 cm^{-3} for soil samples and from 0.040 to 0.053 cm^3 cm^{-3} for substrates. Consequently, the $\theta_m - Raw$ relationship is more effective than the $\theta_m - \varepsilon^{0.5}$ relationship, especially in inorganic soils. In substrates, the CAL method gives lower RMSE values (Tables 2 and 3). The RMSE values for the substrates

using the CAL method range from 0.022 to 0.043 cm^3 cm^{-3}, using the manufacturer's cubic calibration equation they range from 0.058 to 0.096 cm^3 cm^{-3}, and using linear calibration θ_m − Raw they range from 0.040 to 0.053 cm^3 cm^{-3}. These results indicate that the CAL method tends to produce more accurate results for substrates. Also, from Table 3 it can be seen that the parameters a and b of the linear relationship θ_m − Raw have their highest and lowest values in substrates, compared with soils, which reflects the special physicochemical characteristics of the substrates. The coefficients of the θ_m − Raw linear relationships in mineral soils differ from the coefficients of the linear relation presented by Cominelli et al. [25], which shows that the application of one equation, as suggested by Cominelli et al. [25], for all soil types is not effective, a fact that is also confirmed by the RMSE values (Table 3). The θ_m − Raw relationship estimates θ with higher accuracy compared with the physically based model $\theta_m - \varepsilon^{0.5}$, a fact that may be attributed to the fact that the Raw output–ε_a relationship (Equation (8)) for these sensors may need to be recalibrated.

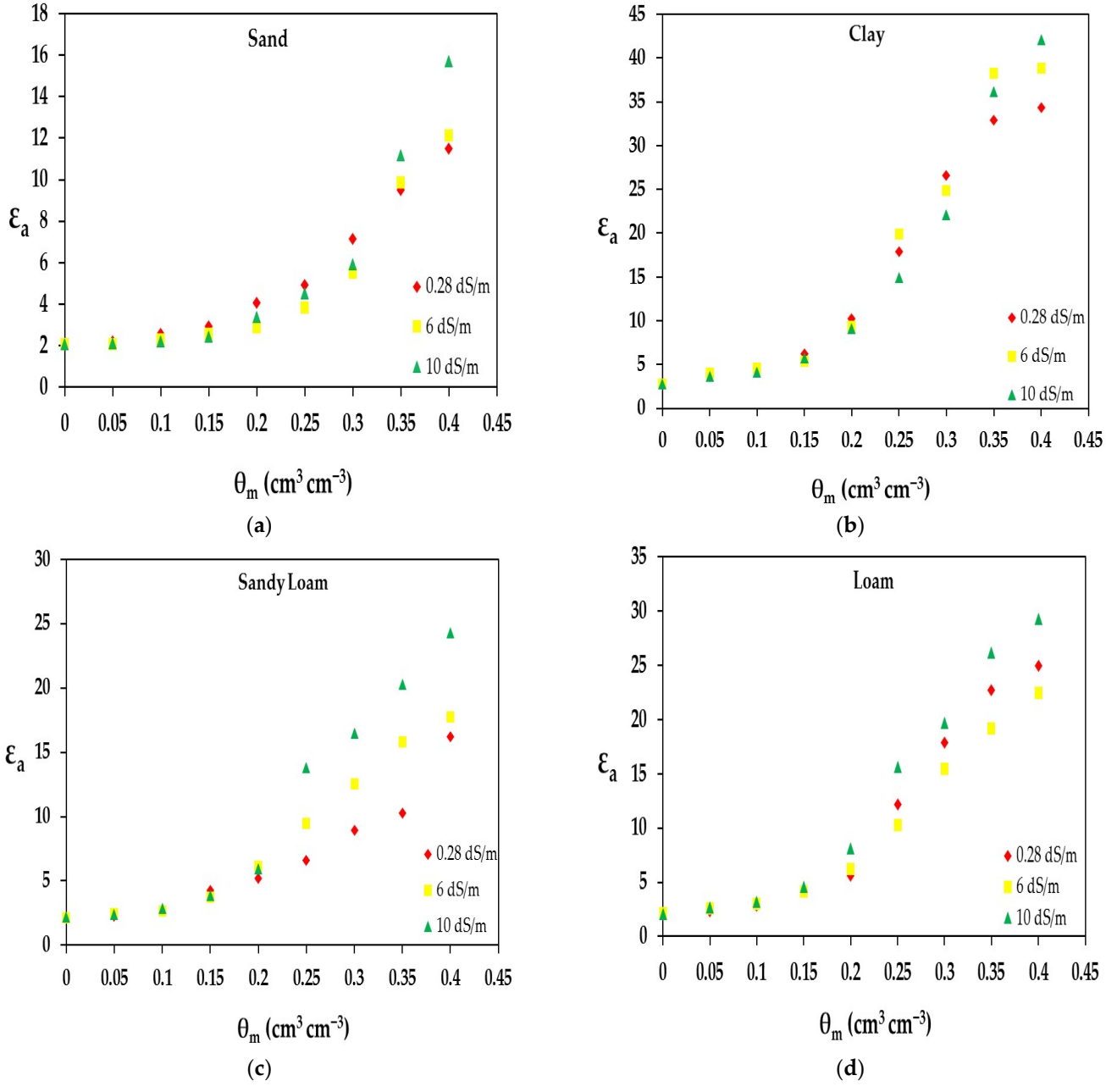


Figure 5. The ε_a − θ_m relationship (point) for (**a**) sand, (**b**) clay, (**c**) sandy loam and (**d**) loam soil samples for all salinity levels for measurements with TEROS 10.

Table 3. Parameters a (slope) and b (interception) of the linear relationship θ-Raw for the studied soil types and substrates given by the linear regression equation, along with R^2 and RMSE values calculated from manufacturer's equation ($\theta - Raw^3$) (Equation (6)), Cominelli's equation (Equation (9)), CAL ($\theta - \varepsilon^{0.5}$) (Table 2) and linear calibration equation ($\theta - Raw$), respectively, for EC = 0.28 dS m^{-1}.

Substrate Type	b	a	R^2	RMSE (Manuf)	RMSE (Cominelli)	RMSE (CAL)	RMSE (Linear)
Sand	-5.66×10^{-1}	5.56×10^{-4}	0.981	0.061	0.063	0.022	0.018
Sandy Loam	-4.89×10^{-1}	4.81×10^{-4}	0.981	0.052	0.046	0.018	0.020
Loam	-4.87×10^{-1}	4.92×10^{-4}	0.974	0.060	0.060	0.040	0.024
Clay	-5.01×10^{-1}	4.68×10^{-4}	0.964	0.046	0.047	0.027	0.028
Silty Clay Loam	-4.83×10^{-1}	4.76×10^{-4}	0.987	0.047	0.044	0.028	0.017
Sandy Clay Loam	-4.08×10^{-1}	3.92×10^{-4}	0.962	0.033	0.027	0.024	0.028
Perlite	-2.63×10^{-1}	3.19×10^{-4}	0.887	0.058	-	0.028	0.040
Peat	-4.74×10^{-1}	5.29×10^{-4}	0.961	0.081	-	0.043	0.044
Stone Wool	-7.37×10^{-1}	6.70×10^{-4}	0.963	0.096	-	0.022	0.053

3.3. Salinity Effects in Soils

In Table 4, the parameter values a (slope) and b (interception) are presented for each soil type and each EC_w level of the $\theta_m - \varepsilon^{0.5}$ relationship, along with the correlation coefficient R^2, respectively. According to our findings, both a and b values are salinity-dependent in all cases. The level of EC_w has an impact on the linearity of the relationship $\theta_m - \varepsilon^{0.5}$ due to the reduction of R^2 as the salinity level increases. This observation emphasizes the need for specific calibration for each soil type and at each salinity level for more accurate estimation of θ.

Table 4. Parameters a (slope) and b (interception) in relationships $\theta - \varepsilon^{0.5}$ for four soil types and three salinity levels, along with R^2 values, respectively, for TEROS 10.

Soil Type	EC_w (dS m^{-1})	b	a	R^2
Sand	0.28	−0.213	0.174	0.964
	6	−0.209	0.197	0.828
	10	−0.104	0.132	0.875
Sandy Loam	0.28	−0.155	0.135	0.980
	6	−0.122	0.124	0.951
	10	−0.108	0.114	0.953
Loam	0.28	−0.118	0.127	0.905
	6	−0.101	0.106	0.956
	10	−0.033	0.089	0.803
Clay	0.28	−0.089	0.080	0.956
	6	−0.067	0.073	0.935
	10	−0.061	0.073	0.935

In Table 5, the parameters a (slope) and b (interception) of the linear regression equation $\theta - Raw$ are given for each soil type and each EC_w, along with the correlation coefficient R^2, respectively. The relationship $\theta - Raw$ is more linear than the equivalent $\theta - \varepsilon^{0.5}$ in soils, due to the fact that $0.896 < R^2 < 0.981$, whereas in relationship $\theta - \varepsilon^{0.5}$ the R^2 values range between 0.803 and 0.980.

As can be seen in Figure 5a, for sand, the values of ε_a for EC_w = 0.28 dS m^{-1} are higher in relation to the corresponding ones for EC_w = 6 or 10 dS m^{-1}, until θ_m = 0.30 cm^3 cm^{-3}, while the opposite is expected due to the low operating frequency of the sensor. This trend also applies to clay (Figure 5), to sandy loam (Figure 5c) and to loam (Figure 5d). From θ = 0.25 cm^3 cm^{-3} and beyond, the obtained values of ε_a for each θ_m are higher at high EC_w values. It appears that this irregularity of the unexpected behavior of the sensor may be attributed to its response to EC_w, which is highly nonlinear and inverse, from negative

to small EC_w to positive to large EC_w as it turns out in aqueous liquids. Additionally, it could be noted the possible contribution of the parameters related to the soil texture to this phenomenon. Specifically, fine-grained soils heavily influence the moisture regime compared with coarse-grained soils as they have smaller particle sizes and a larger surface area relative to their volume.

Table 5. Parameters a (slope) and b (interception) in relationships θ − Raw for four soil types and three salinity levels, along with R^2 values, respectively, for TEROS 10.

Soil Type	EC_w (dS m^{-1})	b	a	R^2
Sand	0.28	-5.66×10^{-1}	5.56×10^{-4}	0.981
	6	-6.00×10^{-1}	6.22×10^{-4}	0.903
	10	-4.37×10^{-1}	4.77×10^{-4}	0.933
Sandy Loam	0.28	-4.89×10^{-1}	4.81×10^{-4}	0.981
	6	-4.51×10^{-1}	4.60×10^{-4}	0.976
	10	-4.28×10^{-1}	4.36×10^{-4}	0.975
Loam	0.28	-4.87×10^{-1}	4.92×10^{-4}	0.974
	6	-4.20×10^{-1}	4.22×10^{-4}	0.980
	10	-3.52×10^{-1}	3.93×10^{-4}	0.896
Clay	0.28	-5.07×10^{-1}	4.68×10^{-4}	0.965
	6	-4.09×10^{-1}	3.72×10^{-4}	0.963
	10	-4.12×10^{-1}	3.79×10^{-4}	0.981

In Table 6, the values of RMSE extracted from the third-order factory calibration equation (Equation (6)) are presented, along with those proposed by Cominelli's calibration equation (Equation (9)), those derived from the CAL method and those from the linear regression calculation (Tables 3 and 5), based on the findings of this study and using Raw values as the predictor variable for θ. The last one has the best performance in soils because RMSE ranges from 0.022 to 0.032 cm^3 cm^{-3} in average scale, almost 50% lower than the equivalent values of the manufacturer's supplied calibration equation. The RMSE values obtained by the CAL method are from 0.025 to 0.041 cm^3 cm^{-3}, while the corresponding values taking into account the manufacturer's calibration range from 0.050 to 0.081 cm^3 cm^{-3}, respectively. Although, the RMSE values obtained by CAL are higher than those of the linear regression method, they are less on average than the threshold value 0.04 cm^3 cm^{-3} [40], with the exception of loam, where RMSE = 0.041. The Cominelli's calibration equation provides RMSE values between 0.046 and 0.084 cm^3 cm^{-3}. The MAE values, by using the third-order factory calibration equation (Equation (6)), range for all studied cases from 0.02 cm^3 cm^{-3} to 0.06 cm^3 cm^{-3} with the exceptions of sand (for EC_w = 6 and 10 dS m^{-1}) and stone wool (EC = 0.28 dS m^{-1}), where an MAE value of 0.08 cm^3 cm^{-3} is obtained for each of the cases above. The MAE values, obtained by the CAL method across the six soils, are almost in agreement with those using linear regression calculation (Tables 3 and 5). Both of them range from 0.01 cm^3 cm^{-3} to 0.04 cm^3 cm^{-3}, with the exception of loam (for EC = 10 dS m^{-1}), where MAE = 0.05 cm^3 cm^{-3}, and are about 50% lower on average than the abovementioned corresponding values. In substrates, the CAL method results in 0.02 cm^3 cm^{-3} < MAE < 0.03 cm^3 cm^{-3}; meanwhile, the linear regression calculation results in 0.04 cm^3 cm^{-3} < MAE < 0.05 cm^3 cm^{-3}. The Cominelli's calibration equation provides MAE values between 0.02 cm^3 cm^{-3} and 0.08 cm^3 cm^{-3} for the six soil types.

Table 6. The RMSE values of θ relative to those calculated using the manufacturer's equation (θ − Raw^3), Cominelli's equation (Equation (9)), CAL equation (θ − $\varepsilon^{0.5}$) and linear calibration equation (θ − Raw).

	Manufacturer Calibration			Cominelli's Equation		CAL		Linear Calibration	
Soil type	**EC_w (dS m^{-1})**	**RMSE**	**Average**	**RMSE**	**Average**	**RMSE**	**Average**	**RMSE**	**Average**
Sand	0.28	0.061	0.081	0.063	0.084	0.022	0.038	0.018	0.032
	6	0.094		0.102		0.047		0.041	
	10	0.088		0.086		0.046		0.038	
Sandy Loam	0.28	0.052	0.051	0.046	0.046	0.018	0.025	0.020	0.022
	6	0.055		0.051		0.028		0.023	
	10	0.046		0.041		0.028		0.023	
Loam	0.28	0.060	0.050	0.060	0.051	0.040	0.041	0.024	0.031
	6	0.030		0.029		0.027		0.021	
	10	0.060		0.064		0.057		0.047	
Clay	0.28	0.046	0.050	0.047	0.047	0.027	0.031	0.028	0.025
	6	0.056		0.052		0.033		0.028	
	10	0.048		0.041		0.033		0.020	
Silty Clay Loam	0.28	0.047		0.044		0.028		0.017	
Sandy Clay Loam	0.28	0.033		0.027		0.024		0.028	
Peat	0.28	0.081		-		0.043		0.044	
Perlite	0.28	0.058		-		0.028		0.040	
Stone Wool	0.28	0.096		-		0.022		0.053	

4. Conclusions

In this study the performance of TEROS 10 sensor was investigated across six soil samples with an extensive array of properties, three substrates used as soilless porous media and also aqueous solutions with increasing EC_w. The most significant results of this study are:

- For all soil samples and different EC_w levels, soil-specific calibration was necessary for more accurate results, especially in high-salinity levels. The third-order manufacturer's calibration equation did not accurately determine θ in cases of increasing soil salinity. The linear calibration procedure (Tables 3 and 5), as evaluated with the RMSE, was the most effective method for all soil types for TEROS 10 compared with the other calibration methods. Cominelli's calibration equation provided an improvement compared with the manufacturer's cubic calibration equation.
- In liquids with increasing EC, there was an irregular behavior of TEROS 10 due to the strong effect of EC_w, which was highly nonlinear with a reversed direction, from negative at small EC_w to positive at large.
- An unusual phenomenon was observed in most soil samples, specifically at low and moderate salinity levels (from θ_m = 0 to θ_m = 0.20 cm^3 cm^{-3}). The values of ε_a were not affected by the increasing EC_w of the samples, and the readings of TEROS 10 were higher for EC_w = 0.28 than for EC_w = 6 and 10 dS m^{-1}. It must be highlighted that in sand and clay this phenomenon lasted until θ_m = 0.30 dS m^{-1}. From θ_m = 0.25 cm^3 cm^{-3} and beyond, there was a clear separation of the obtained values of ε_a, the increase of which followed the increasing EC_w level.
- The CAL procedure seems to be the most effective calibration method for soilless porous media. A need for a specific calibration of the sensor device in substrates is necessary if the goal is the most accurate estimation of their moisture content.

Author Contributions: Conceptualization, A.F., D.L. and G.K.; methodology, A.F., D.L. and G.K.; prototyping, D.L.; software, D.L.; validation, A.F., D.L. and G.K.; investigation, A.F. and D.L.; data curation, A.F. and D.L.; writing—original draft preparation, A.F., D.L. and G.K.; writing—review and

editing, A.F., D.L., G.K. and K.G.A.; visualization, A.F. and D.L.; supervision, G.K. and K.G.A. All authors have read and agreed to the published version of the manuscript.

Funding: This research received no external funding.

Data Availability Statement: Available upon request.

Conflicts of Interest: The authors declare no conflicts of interest.

References

1. Liu, Y.; Ma, X.; Shu, L.; Hancke, G.P.; Abu-Mahfouz, A.M. From industry 4.0 to agriculture 4.0: Current status, enabling technologies, and research challenges. *IEEE Trans. Ind. Inform.* **2020**, *17*, 4324–4334. [CrossRef]
2. Soulis, K.; Elmaloglou, S. Optimum soil water content sensors placement for surface drip irrigation scheduling in layered soils. *Comput. Electron. Agric.* **2018**, *152*, 1–8. [CrossRef]
3. Dobriyal, P.; Qureshi, A.; Badola, R.; Hussain, S.A. A review of the methods available for estimating soil moisture and its implications for water resource management. *J. Hydrol.* **2012**, *458*, 110–117. [CrossRef]
4. Rosenzweig, C.; Elliott, J.; Deryng, D.; Ruane, A.C.; Müller, C.; Arneth, A.; Boote, K.J.; Folberth, C.; Glotter, M.; Khabarov, N.; et al. Assessing agricultural risks of climate change in the 21st century in a global gridded crop model intercomparison. *Proc. Natl. Acad. Sci. USA* **2014**, *111*, 3268–3273. [CrossRef]
5. Dong, Y.; Miller, S.; Kelley, L. Performance evaluation of soil moisture sensors in coarse- and fine-textured michigan agricultural soils. *Agriculture* **2020**, *10*, 598. [CrossRef]
6. Doungmanee, P. The nexus of agricultural water use and economic development level. *Kasetsart J. Soc. Sci.* **2016**, *37*, 38–45. [CrossRef]
7. Hassoun, A.; Marvin, H.J.P.; Bouzembrak, Y.; Barba, F.J.; Castagnini, J.M.; Pallarés, N.; Rabail, R.; Aadil, R.M.; Bangar, S.P.; Bhat, R.; et al. Digital transformation in the agri-food industry: Recent applications and the role of the COVID-19 pandemic. *Front. Sustain. Food Syst.* **2023**, *7*, 1217813. [CrossRef]
8. Topp, G.C.; Davis, J.L.; Annan, A.P. Electromagnetic determination of soil water content: Measurements in coaxial transmission lines. *Water Resour. Res.* **1980**, *16*, 574–582. [CrossRef]
9. Ferre, P.A.; Topp, G.C. Time domain reflectometry. In *Methods of Soil Analysis*; Dane., J.H., Topp, G.C., Eds.; Part 4, Physical Methods; Soil Science Society of America: Madison, WI, USA, 2002; pp. 434–446.
10. Seyfried, M.S.; Grant, L.E.; Du, E.; Humes, K. Dielectric Loss and Calibration of the Hydra Probe Soil Water Sensor. *Vadose Zone J.* **2005**, *4*, 1070–1079. [CrossRef]
11. Kargas, G.; Kerkides, P. Water content determination in mineral and organic porous media by ML2 theta probe. *Irrig. Drain.* **2008**, *57*, 435–449. [CrossRef]
12. Topp, G.C.; Reynolds, W.D. Time domain reflectometry: A seminal technique for measuring mass and energy in soil. *Soil Tillage Res.* **1998**, *47*, 125–132. [CrossRef]
13. Kargas, G.; Soulis, K. Performance evaluation of a recently developed soil water content, dielectric permittivity, and bulk electrical conductivity electromagnetic sensor. *Agric. Water Manag.* **2019**, *213*, 568–579. [CrossRef]
14. Nasta, P.; Coccia, F.; Lazzaro, U.; Bogena, H.R.; Huisman, J.A.; Sica, B.; Mazzitelli, C.; Vereecken, H.; Romano, N. Temperature-Corrected Calibration of GS3 and TEROS-12 Soil Water Content Sensors. *Sensors* **2024**, *24*, 952. [CrossRef]
15. Wyseure, G.; Mojid, M.A.; Manzoor, A.M. Measurement of volumetric water content by TDR in saline soils. *Eur. J. Soil Sci.* **2005**, *48*, 347–354. [CrossRef]
16. Robinson, D.A.; Jones, S.B.; Wraith, J.M.; Or, D.; Friedman, S.P. A Review of Advances in Dielectric and Electrical Conductivity Measurement in Soils Using Time Domain Reflectometry. *Vadose Zone J.* **2003**, *2*, 444–475. [CrossRef]
17. Schwartz, R.C.; Casanova, J.; Pelletier, M.; Evett, S.; Baumhardt, R. Soil Permittivity Response to Bulk Electrical Conductivity for Selected Soil Water Sensors. *Vadose Zone J.* **2013**, *12*, 1–13. [CrossRef]
18. Mohamed, A.-M.O.; Paleologos, E.K. Dielectric Permittivity and Moisture Content. In *Fundamentals of Geoenvironmental Engineering*; Mohamed, A.-M.O., Paleologos, E.K., Eds.; Butterworth-Heinemann: Oxford, UK, 2018; Chapter 16; pp. 581–637.
19. Qi, Q.; Yang, H.; Zhou, Q.; Han, X.; Jia, Z.; Jiang, Y.; Chen, Z.; Hou, L.; Mei, S. Performance of Soil Moisture Sensors at Different Salinity Levels: Comparative Analysis and Calibration. *Sensors* **2024**, *24*, 6323. [CrossRef]
20. Delta-T Devices. Available online: https://delta-t.co.uk/wp-content/uploads/2017/02/ML3-user-manual-version-2.1.pdf (accessed on 2 April 2024).
21. Meter Group. Available online: https://publications.metergroup.com/Manuals/20587_TEROS11-12_Manual_Web.pdf (accessed on 2 April 2024).
22. Topp, G.C.; Parkin, G.W.; Ferre, P.A. *Soil Water Content in Soil Sampling and Methods of Analysis*, 2nd ed.; Carter, M.R., Gregorich, E.R., Eds.; Canadian Society of Soil Science: Vancouver, BC, Canada, 2008; pp. 939–961.

23. Peranić, J.; Čeh, N.; Arbanas, Z. The Use of Soil Moisture and Pore-Water Pressure Sensors for the Interpretation of Landslide Behavior in Small-Scale Physical Models. *Sensors* **2022**, *22*, 7337. [CrossRef]
24. Millán, S.; Montesinos, C.; Campillo, C. Evaluation of Different Commercial Sensors for the Development of Their Automatic Irrigation System. *Sensors* **2024**, *24*, 7468. [CrossRef] [PubMed]
25. Cominelli, S.; Rivera, L.D.; Brown, W.G.; Ochsner, T.E.; Patrignani, A. Calibration of TEROS 10 and TEROS 12 electromagnetic soil moisture sensors. *Soil Sci. Soc. Am. J.* **2024**, *88*, 2104–2122. [CrossRef]
26. Meter Group. User Guide for TEROS 10. Available online: https://publications.metergroup.com/Manuals/20788_TEROS10_Manual_Web.pdf (accessed on 2 April 2024).
27. Fragkos, A.; Loukatos, D.; Kargas, G.; Arvanitis, K.G. Response of the TEROS 12 Soil Moisture Sensor under Different Soils and Variable Electrical Conductivity. *Sensors* **2024**, *24*, 2206. [CrossRef]
28. Loukatos, D.; Fragkos, A.; Kargas, G.; Arvanitis, K.G. Implementation and Evaluation of a Low-Cost Measurement Platform over LoRa and Applicability for Soil Monitoring. *Future Internet* **2024**, *16*, 443. [CrossRef]
29. Fragkos, A.; Loukatos, D.; Kargas, G.; Symeonaki, E.; Arvanitis, K.G. Assessment of the TEROS 10 and TEROS 12 sensors in soil moisture measurement. *E3S Web Conf.* **2024**, *551*, 03005. [CrossRef]
30. peatman.eu. Available online: https://peatman.eu/neutralized-peat-for-landscaping-ptn-2-0/ (accessed on 2 April 2024).
31. perlite-hellas.gr. Available online: https://perlite-hellas.gr/en/service/ (accessed on 2 April 2024).
32. grodan.com. Available online: https://www.grodan.com/global/solutions/product-overview/vegetable-solutions/grodan-classic-my/ (accessed on 2 April 2024).
33. Nurgul, K.; Ertan, Y.; Üstün, Ş.; Metin, T.; Melek, E.; Selda, O.; Raziye, K.; Hüsnü, Ü.; Halime, Ü. Chapter 5—Peat Use in Horticulture. In *Peat*; Topcuoğlu, B., Turan, M., Eds.; InTech: London, UK, 2018; Chapter 5; pp. 75–90.
34. Markoska, V.; Spalevic, V.; Gulaboski, R. A research on the influence of porosity on perlite substrate and its interaction on porosity of two types of soil and peat substrate. *Agric. For.* **2018**, *64*, 15–29. [CrossRef]
35. O'Kelly, B.C.; Sivakumar, V. Water Content Determinations for Peat and Other Organic Soils Using the Oven-Method. *Dry. Technol.* **2014**, *32*, 631–643. [CrossRef]
36. Seyfried, M.S.; Murdock, M.D. Measurement of soil content with a 50 MHz soil dielectric sensor. *Soil Sci. Soc. Am. J.* **2004**, *68*, 394–403.
37. Hilhorst, M.A. A pore water conductivity sensor. *Soil Sci. Soc. Am. J.* **2000**, *64*, 1922–1925. [CrossRef]
38. Kargas, G.; Kerkides, P.; Seyfried, M.S. Response of Three Soil Water Sensors to Variable Solution Electrical Conductivity in Different Soils. *Vadose Zone J.* **2014**, *13*, 1–13. [CrossRef]
39. Rosenbaum, U.; Huisman, J.A.; Vrba, I.; Vereecken, H.; Bogena, H.R. Correction of temperature and electrical conductivity effects on dielectric permittivity measurements with ECH2O sensors. *Vadose Zone J.* **2011**, *10*, 582–593. [CrossRef]
40. Cosh, M.H.; Ochsner, T.E.; McKee, L.; Dong, J.; Basara, J.B.; Evett, S.R.; Hatch, C.E.; Small, E.E.; Steele-Dunne, S.C.; Zreda, M.; et al. The Soil Moisture Active Passive Marena, Oklahoma, In Situ Sensor Testbed (SMAP-MOISST): Testbed Design and Evaluation of In Situ Sensors. *Vadose Zone J.* **2016**, *15*, 1–11. [CrossRef]

Disclaimer/Publisher's Note: The statements, opinions and data contained in all publications are solely those of the individual author(s) and contributor(s) and not of MDPI and/or the editor(s). MDPI and/or the editor(s) disclaim responsibility for any injury to people or property resulting from any ideas, methods, instructions or products referred to in the content.